# C-vector for identification of oceanic secondary circulations across Arctic Fronts in Fram Strait

Peter C. Chu

Naval Ocean Analysis and Prediction Laboratory, Department of Oceanography, Naval Postgraduate School, Monterey, USA

Received 25 July 2002; accepted 28 August 2002; published 19 December 2002.

[1] Secondary circulation, referring to the motion relative to a basic flow (geostrophic and hydrostatic balanced), occurs often in the ocean such as deep convection and circulations driven by fronts and eddies. It affects the general circulation and the mass, heat, salt, and energy balance. The oceanic secondary circulation is difficult to measure directly, but is easy to be identified by pseudovorticity using routine observations. A C-vector method, commonly used in atmospheric mesoscale moist frontogenesis, is applied to oceanography for identifying frontal secondary circulation in Fram Strait using Conductivity-Temperature-Depth data collected during a large-scale hydrographic survey on R/V Valdivia cruise-54 of the eastern Greenland Sea and Fram Strait from 16 March to 5 April 1987. Possible application of this method to large-scale motion is also discussed. *INDEX TERMS:* 4528 Oceanography: Physical: Fronts and jets; 4207 Oceanography: General: Arctic and Antarctic oceanography; 4279 Oceanography: General: Upwelling and convergences; 4520 Oceanography: Physical: Eddies and mesoscale processes. **Citation:** Chu, P. C., C-vector for identification of oceanic secondary circulations across Arctic Fronts in Fram Strait, *Geophys. Res. Lett.*, *29*(24), 2157, doi:10.1029/2002GL015978, 2002.

## 1. Introduction

[2] Fram Strait (Figure 1) is the only deep connection between the Arctic Ocean and the rest of the world ocean through the Greenland Sea, Iceland Sea, and Norwegian Sea (GIN Sea). The different water masses encountered in the GIN Sea and Fram Strait often form fronts. The Arctic front or frontal zone is oriented more or less meridiona11y. It separates the warm and salty North Atlantic Water (NAW) in the Norwegian and West Spitsbergen currents from the cooler and fresher Arctic Water (AW) [*Dietrich*, 1969]. After analyzing hydrographic data along 74°45′N in February 1989 during cruise VA78 of R/V Valdivia, *van Aken et al.* [1991] identified four Arctic fronts south of Fram Strait.The physical-biological effect arises from the significant vertical component of the 3D ageostrophic flow (or called the secondary circulation) associated with the fronts, where vertical upward motion may act as a fertilizer of the upper water column. A better knowledge of the secondary circulation is therefore crucial. However, direct measurement of the secondary circulation in the ocean is difficult.

## 2. C-Vector

[3] Let $(x, y)$ be the horizontal coordinates and $z$ the vertical coordinate. With the Boussinesq approximation, the geostrophic velocity $(u_g, v_g)$ is related to the density through the thermal wind relation,

$$f\frac{\partial u_g}{\partial z} = -\frac{\partial b}{\partial y},\ f\frac{\partial v_g}{\partial z} = \frac{\partial b}{\partial x},\ b = -g\frac{\hat{\rho}}{\rho_0} \tag{1}$$

where $\hat{\rho} = \rho - \rho_0$, and $(\rho, \rho_0)$ are the in-situ density and characteristic density. The variable $b$ is usually called the buoyancy. The total flow, $\boldsymbol{V} = (u, v, w)$, is decomposed into geostrophic and ageostrophic parts: $\mathbf{V} = \mathbf{V}_g + \mathbf{V}_{ag}$. If the advection of momentum and buoyancy is dominated by the geostrophic advection (i.e., quasi-geostrophic system),

$$\mathbf{V}\bullet\nabla\mathbf{V} \approx \mathbf{V}_g\bullet\nabla\mathbf{V}_g, \quad \mathbf{V}\bullet\nabla b \approx \mathbf{V}_g\bullet\nabla b, \tag{2}$$

the ageostrophic velocity is determined by

$$-fv_{ag} = \frac{1}{\rho_0}\frac{\partial X}{\partial z} - \left(\frac{\partial}{\partial t} + \mathbf{V}_g\bullet\nabla\right)u_g, \tag{3}$$

$$fu_{ag} = \frac{1}{\rho_0}\frac{\partial Y}{\partial z} - \left(\frac{\partial}{\partial t} + \mathbf{V}_g\bullet\nabla\right)v_g, \tag{4}$$

$$N^2 w_{ag} = \frac{\partial B}{\partial z} - \left(\frac{\partial}{\partial t} + \mathbf{V}_g\bullet\nabla\right)b, \tag{5}$$

where $(X, Y)$ and $B$ are the vertical turbulent momentum and buoyancy fluxes (downward positive), and $N$ is the Brunt-Vaisala frequency.

[4] Cross derivatives among (3)–(5) lead to the definition of pseudovorticity [*Xu*, 1992],

$$\frac{\partial}{\partial y}\left(N^2 w_a\right) - \frac{\partial}{\partial z}\left(f^2 v_a\right) = 2C_x, \tag{6a}$$

$$\frac{\partial}{\partial z}\left(f^2 u_a\right) - \frac{\partial}{\partial x}\left(N^2 w_a\right) = 2C_y, \tag{6b}$$

$$\frac{\partial}{\partial x}\left(f^2 v_a\right) - \frac{\partial}{\partial y}\left(f^2 u_a\right) = 2C_z, \tag{6c}$$

where

$$C_x = -f\frac{\partial(u_g, v_g)}{\partial(y, z)} + \frac{1}{2}\frac{\partial}{\partial z}\left(f\frac{\partial X}{\partial z} + \frac{\partial B}{\partial y}\right), \tag{7a}$$

$$C_y = -f\frac{\partial(u_g, v_g)}{\partial(z, x)} + \frac{1}{2}\frac{\partial}{\partial z}\left(f\frac{\partial Y}{\partial z} - \frac{\partial B}{\partial x}\right), \tag{7b}$$


0094-8276/02/2002GL015978$05.00

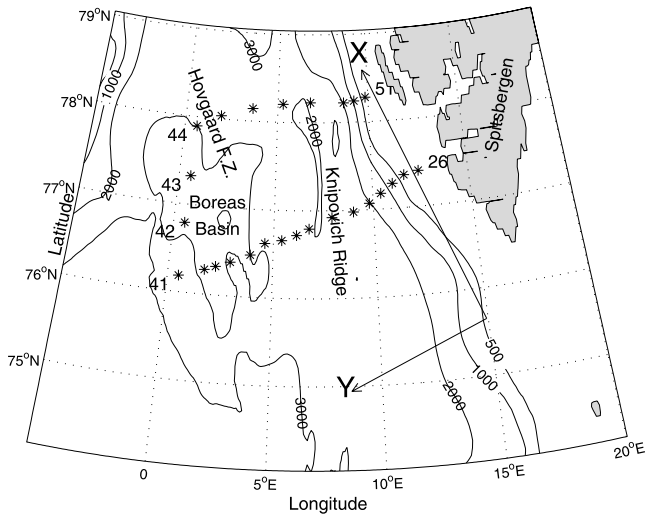


**Figure 1.** Geography of East Fram Strait, coordinate system, and CTD stations of R/V Valdivia cruise 54 in Fram Strait from March 16 to April 5, 1987.

$$C_z = -f\frac{\partial(u_g, v_g)}{\partial(x,y)} - \frac{f}{2}\frac{\partial}{\partial z}\left(\frac{\partial X}{\partial x} + \frac{\partial Y}{\partial y}\right) - \frac{\beta}{2}\frac{\partial Y}{\partial z}, \qquad (7c)$$

are components of C-vector. Thus, the pseudovorticity of the secondary circulation is determined by three forcing factors: (a) geostrophic forcing (i.e., distinct water masses across the front), $-f\partial(u_g, v_g)/\partial(y,z)$, $-f\partial(u_g, v_g)/\partial(z,x)$, $-f\partial(u_g, v_g)/\partial(x,y)$, (b) turbulent momentum flux ($X$, $Y$), and (c) buoyancy flux ($B$). In the upper ocean, the last two factors are mainly caused by the surface wind stress and buoyancy flux. As pointed by *Xu* [1992], the C-vector is the ageostrophic vortex line (Figure 2) whose horizontal components ($C_x$, $C_y$) represent the secondary circulation in vertical cross-section.

[5] Observations show generally well-mixed upper ocean by turbulent motion. The transition between the turbulent mixed layer and the stratified water below is a thin entrainment zone with large gradients of density and velocity. All turbulent fluxes are usually assumed to vanish below the ocean mixed layer. The mixed layer depth $h$ is defined as the depth above which temperature, salinity, or velocity (geostrophic plus ageostrophic) is vertically uniform to certain critical value. The vertical uniformity leads to the bulk model parameterization [e.g., *Price et al.*, 1986; *Chu et al.*, 1990; *Chu and Garwood*, 1991] of turbulent fluxes ($X$, $Y$, $B$)

$$(X, Y) = (\tau_x, \tau_y) + \left[(\tau_x, \tau_y) - (X, Y)_{-h}\right]\frac{z}{h},$$

$$B = B_0 + (B_0 - B_{-h})\frac{z}{h}, \qquad \text{for } z > -h, \qquad (8a)$$

$$(X, Y, B) \simeq 0 \qquad \text{for } z < -h, \qquad (8b)$$

where ($\tau_x$, $\tau_y$) is the surface wind stress, and $B_0$ is the surface buoyancy flux. $(X, Y)_{-h}$ and $B_{-h}$ are turbulent fluxes at the base of mixed layer, which are computed from the surface fluxes. From (8a) and (8b) we obtain

$$\frac{\partial^2 X}{\partial z^2} = 0, \ \frac{\partial^2 Y}{\partial z^2} = 0, \qquad (9)$$

for the whole water column.

[6] Since $B$ is a linear function of $z$ in the surface mixed layer [see (8a)], the contribution of $B$ to ($C_x$, $C_y$) in the surface mixed layer is depth-independent [see (8a)]. Since $B_{-h}$ is computed from the surface turbulent fluxes ($\tau_x$, $\tau_y$) and $B_0$ (bulk models), the atmosphere may control the scale of the horizontal variability of $B_{-h}$ and $B_0$. The atmosphere has most of its energy in scales of several hundreds of kilometers and longer, it is reasonable to assume that

$$\frac{\partial}{\partial z}\left(\frac{\partial B}{\partial y}\right) = 0, \quad \frac{\partial}{\partial z}\left(\frac{\partial B}{\partial x}\right) = 0, \qquad (10)$$

across the Arctic front, and therefore the horizontal C-vector components are computed from the geostrophic forcing only. The geostrophic forcing has been recognized as the major factor to cause the atmospheric frontal secondary circulation [*Hoskins et al.*, 1978; *Xu*, 1992]. It may also be important for oceanic frontal secondary circulation.

## 3. Data

[7] Conductivity-Temperature-Depth (CTD) data, collected during a large-scale hydrographic survey on RV/VALDIVIA cruise-54 of the eastern Greenland Sea and Fram Strait from 16 March to 5 April 1987 [*Quadfasel and Ungewiss*, 1988], are used to illustrate the advantage of using the C-vector method in analyzing oceanic secondary circulation. Along seven sections a total of 73 CTD profiles were taken (Figure 1). Four of these sections crossed the Arctic Front that separates the Greenland Sea gyres from the warm and saline northward flowing Norwegian Atlantic Current and the West Spitsbergen Current. The sections were designed to form three closed boxes to allow calculation of transport budgets. Usual station spacing was 56 km except along Fram Strait section at 78° 25′N and across the Hovgaard Fracture Zone, where the spacing was decreased to less than 28 km. All CTD profiles were run to within 5 m of the bottom.

## 4. Potential Density

[8] The potential density excess referred to 500 db computed from the CTD data shows the existence of multi-frontal zones in Fram Strait. For example, three Arctic

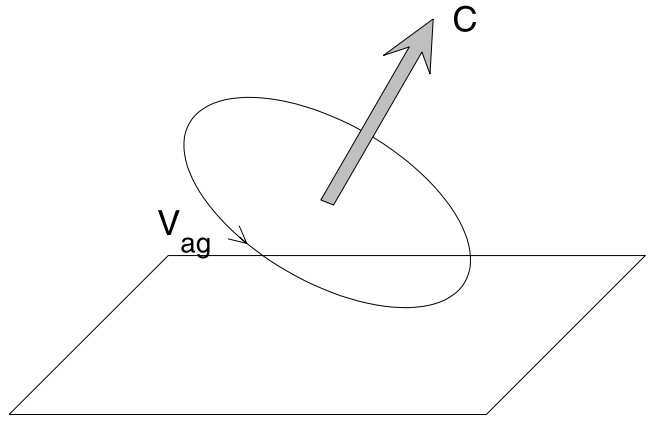


**Figure 2.** C-vector and the secondary circulation.

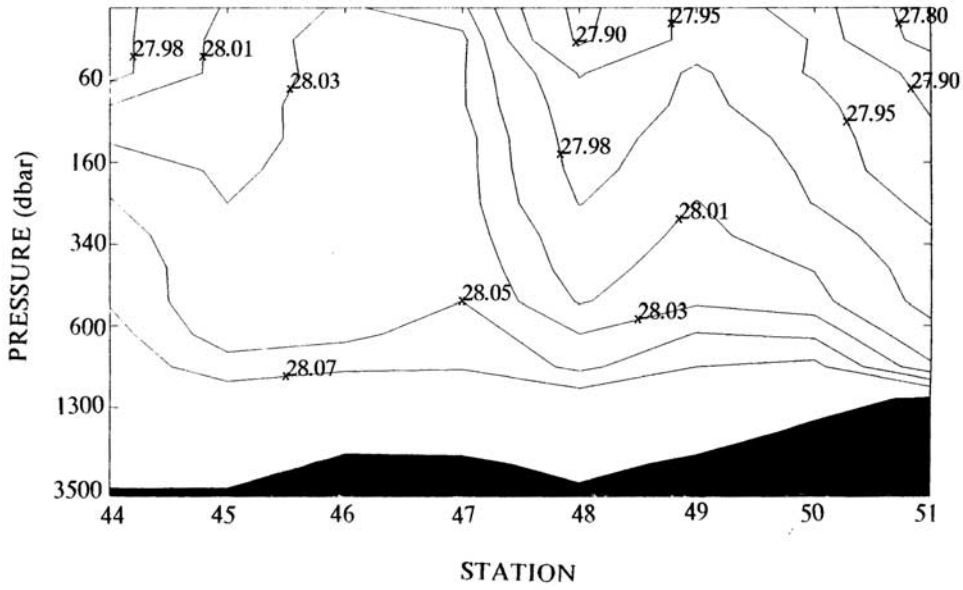


**Figure 3.** Potential density excess referred to 500 db along the north cross-section in Fram Strait (from Stations 44–51).

fronts are identified from the north cross section (Stations 44 to 51) (Figure 3): (a) eastern front occurring near the west coast of Spitsbergen (Stations 49–51), (b) shallow western front (above 160 m depth) occurring near 0° longitude (Stations 44–46) in the Hovgaard Fracture Zone, and (c) a deep mid-front (Stations 47–48) in the north Knipovich Ridge. In the south cross-section in Fram Strait (Stations 26–41, Figure 4), only two fronts can be identified with a strong and shallow front in the Boreas Basin (Stations 34–36) and a weak deep front near the west coast of Spitsbergen (Stations 26–30).

## 5. Horizontal Pseudovorticity

[9] Taking 2500 db as the reference level, the geostrophic current $(u_g, v_g)$ is computed from density, and then the horizontal components of the C-vector are computed from $(u_g, v_g)$. Figure 5 shows the $x$-component of the non-dimensional pseudovorticity $(C_x/f^2)$ along the north cross section (Stations 44 to 51). Looking toward north the positive (negative) values of $C_x/f^2$ imply a clockwise (anticlockwise) circulation. Two clockwise and two anti-clockwise secondary circulations are identified. Among them, the clockwise secondary circulations are deeper than the anticlockwise secondary circulations (depth less than 60 m). Note that in this study, the geostrophic current is computed as 2500 db to be assumed as the level of no motion. This may affect the C-vector computation especially in large horizontally sheared barotropic current such as in Fram Strait [*Fahrbach et al.*, 2001]. However, Figure 5 keeps almost the same as 2000 db is chosen as the reference level.

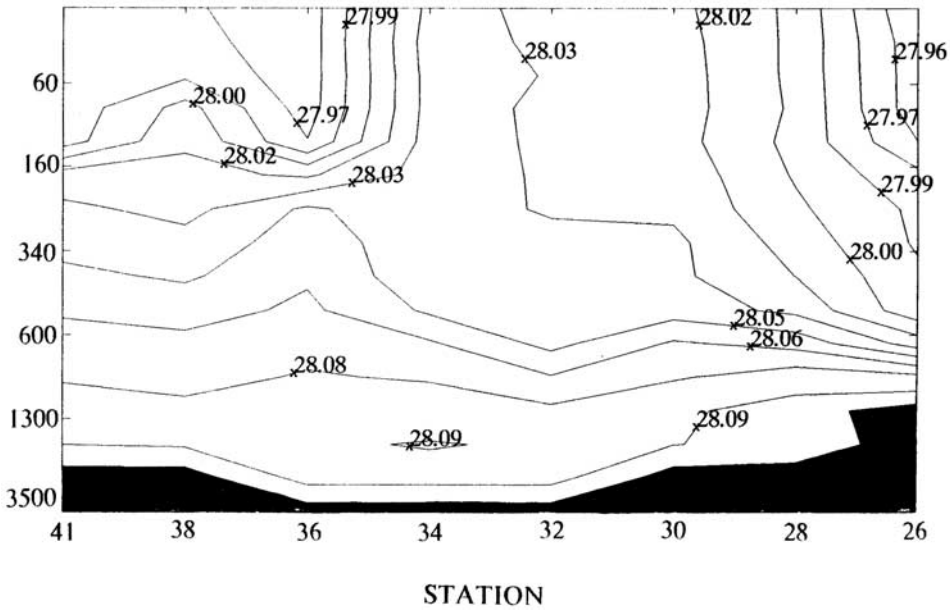


**Figure 4.** Potential density excess referred to 500 db along the south cross-section in Fram Strait (from Stations 26–41).

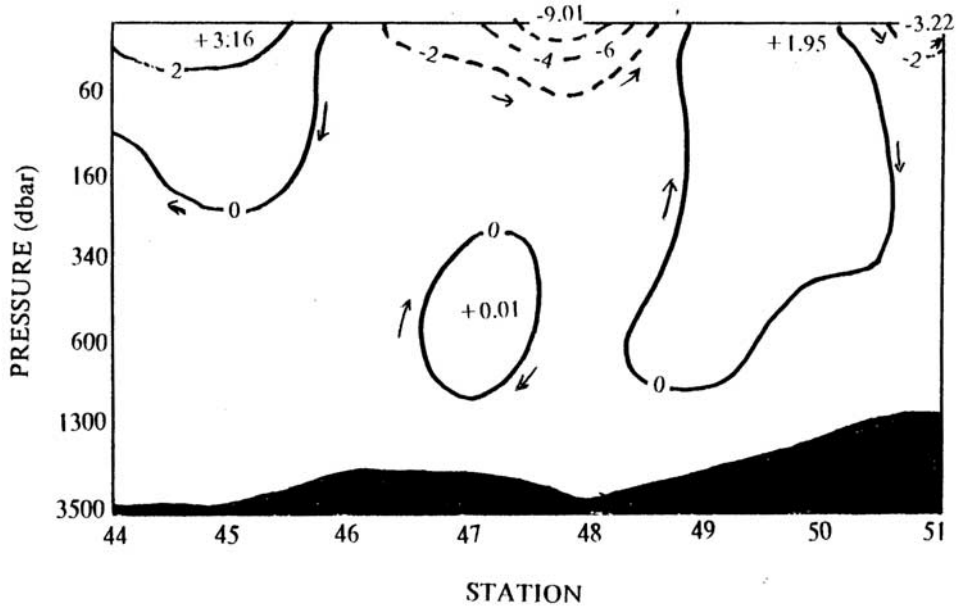


**Figure 5.** Nondimensional horizontal pseudovorticity, $C_x/f^2$, along the north cross-section in Fram Strait (from Stations 44–51).

[10] The most striking feature is the existence of a shallow (surface to 60 m), strong anticlockwise secondary circulation with a minimum value of $C_x/f^2$ around −9.01, located near the Knipovich Ridge (Stations 46–48). We may call it the Knipovich cell. Its upward and downward branches are connected to two clockwise secondary cells from the east (upward branch) and west (downward branch). Below the Knipovich cell between 340 and 1000 m depth, there is a very weak clockwise vorticity (a maximum value of $C_x/f^2$ around 0.01).

[11] East of the Knipovich cell, a deep (surface to 1000 m), clockwise secondary circulation with a maximum pseudovorticity of 1.95 is identified near the West Spitsbergen slope (Stations 48–50). We may call it the West Spitsbergen cell. Its downward branch follows the slope. Its upward branch connects to the Knipovich cell. West of the Knipovich cell, a relatively shallow (to 250 m depth), clockwise secondary circulation with a maximum pseudovorticity of 3.16 is identified in the Hovgaard Fracture Zone (Stations 44–46). Downward branch connects to the Knipovich cell (Stations 46–48). The upward branch is located at Stations 44–45. We may call it the Hovgaard cell. Since the horizontal pseudovorticity ($C_x/f^2$) represents the secondary circulation around the $x$-axis. The larger the $C_x/f^2$, the stronger the secondary circulation is. Strong upwelling is identified between the Knipovich Ridge and the West Spitsbergen slope.

## 6. Conclusions

[12] This paper illustrates the usefulness of the C-vector method in identifying the secondary circulations in Fram Strait frontal zone. However, this method might be used to diagnose the large-scale motion such as the thermohaline circulation represented by the horizontal components ($C_x$, $C_y$) and the wind-driven circulation represented by the vertical component $C_z$. The overturning streamfunction can be obtained from ($C_x$, $C_y$) by solving the Poisson equation with the C-vector components as the forcing terms.

[13] **Acknowledgments.** The author would like to thank Detlef Quadfasel and Manfred Ungewiss for providing the CTD data from R/V Valdivia cruise 54 for the GIN Sea and Fram Strait in March–April 1987 during the Maginal Ice Zone Experiment (MIZEX)-1987. The Office of Naval Research, Naval Oceanographic Office, and Naval Postgraduate School sponsored this research.

## References

Chu, P. C., and R. W. Garwood Jr., On the two-phase thermodynamics of the coupled cloud-ocean mixed layer, *J. Geophys. Res.*, *96*, 3425–3436, 1991.

Chu, P. C., R. W. Garwood Jr., and P. Muller, Unstable and damped modes in coupled ocean mixed layer and cloud models, *J. Marine Syst.*, *1*, 1–11, 1990.

Dietrich, G., Atlas of the hydrography of the northern North Atlantic Ocean, *International Council for the Expedition of the Sea*, Copenhagen, *140*, 1969.

Fahrbach, E., J. Meincke, S. Osterhus, G. Rohardt, U. U. Schauer, V. Tverberg, and J. Verduin, Direct measurements of volume transports through Fram Strait, *Polar Res.*, *20*, 217–224, 2001.

Hopkins, T. S., The GIN Sea, Review of physical oceanography and literature from 1972, *Earth Sci. Rev.*, *30*, 175–318, 1991.

Hoskins, B. J., I. Draghici, and H. C. Davies, A new look at the ω-equation, *Quart. J. Roy. Meteor. Soc.*, *104*, 31–38, 1978.

Price, J. F., R. A. Weller, and R. Pinkel, Diurnal cycling: Observations and models of the upper ocean response to diurnal heating, cooling and wind mixing, *J. Geophys. Res.*, *91*, 8411–8427, 1986.

Quadfasel, D., J.-C. Gascard, and K.-P. Koltermann, Large-scale Oceanography in Fram Strait during the 1984 marginal ice zone experiment, *J. Geophys. Res.*, *92*, 6719–6728, 1987.

van Aken, H. M., D. Quadfasel, and A. Warpakowski, The Arctic front in the Greenland Sea during February 1989: hydrographic and biological observations, *J. Geophys. Res.*, *96*, 4739–4750, 1991.

Xu, Q., Ageostrophic pseudovorticity and geostrophic c-vector forcing - a new look at the Q vector in three dimensions, *J. Atmos. Sci.*, *49*, 981–990, 1992.

P. C. Chu, Naval Ocean Analysis and Prediction Laboratory, Department of Oceanography, Naval Postgraduate School, Monterey, CA 93943, USA.